

Research on Collision Risk Between Light Unmanned Aerial Vehicles and Aircraft Windshield

ZHANG Zhuguo^{1,3}, LU Xiaohua^{2*}, ZHANG Yingchun³, LI Yulong¹, ZHANG Honghai²

1. School of Aeronautics, Northwestern Polytechnical University, Xi'an 710072, P. R. China;

2. College of Civil Aviation, Nanjing University of Aeronautics and Astronautics, Nanjing 211106, P. R. China;

3. Shanghai Aircraft Airworthiness Certification Center, Shanghai 200335, P. R. China

(Received 12 December 2022; revised 7 June 2023; accepted 8 July 2023)

Abstract: With the increasing unmanned aerial vehicles (UAVs) applications, quite a few major aviation incidents and dangerous symptoms have occurred in the vicinity of the airport and the airspace, and air transportation safety is facing a huge potential threat from unorder flight of UAVs. An important aspect regarding the collision risk between a typical UAV and the windshield of a commercial aircraft is investigated. The damage classification and corresponding impact energy range considering the weakest area on the aircraft windshield are obtained via finite element simulation under the most severe condition. According to the simulation results, the damage severity rank can be classified conservatively. In the absence of intervention from air traffic control, Monte Carlo simulation is performed to obtain the collision probability between a UAV and an aircraft with their independent motions by considering the joint constraints of the minimum horizontal safety separation, the minimum lateral safety separation, and the minimum vertical safety separation. In addition, the collision probability levels are also estimated. Based on various combinations of damage severity classifications and collision probability levels, a more conservative qualitative risk matrix is defined regarding collision between a UAV and an aircraft windshield. In general, the results indicate that the collision risk and damage severity are low when the UAV and the aircraft are flying at the height of less than 120 m and a distance of over 3 600 m on the condition of a typical heading angle and a pitch angle, otherwise these factors become serious. This investigation would provide a theoretical basis and practical reference for the normative design and manufacture of UAVs, the policy formulation by authorities on UAV operation control, as well as the risk assessment of UAVs and manned aircraft operating in the same airspace.

Key words: unmanned aerial vehicle (UAV); aircraft windshield; collision probability; damage severity; energy level; risk matrix

CLC number: V279;V328;X949

Document code: A

Article ID: 1005-1120(2023)05-0534-13

0 Introduction

Currently, unmanned aerial vehicles (UAVs) are widely employed in various fields, such as plant protection, electric power inspection, emergency and disaster mitigation, meteorological monitoring, resource surveying, traffic patrolling, ecological mapping, aerial photography, logistics transportation, and municipal administration. With the exten-

sive application of UAVs, new issues have emerged. One of the major hazard is the collision threat on manned aircraft flying in the same airspace because of the unorderly flight of UAVs. Systematic research and empirical studies on the consequences of the collision threat have been conducted in the United States^[1-2]. Investigating the collision or dangerous approaching incidents of UAVs and aircraft publicly reported worldwide, several collision and

*Corresponding author, E-mail address: luxiaohua@nuaa.edu.cn.

How to cite this article: ZHANG Zhuguo, LU Xiaohua, ZHANG Yingchun, et al. Research on collision risk between light unmanned aerial vehicles and aircraft windshield[J]. Transactions of Nanjing University of Aeronautics and Astronautics, 2023, 40(5): 534-546.

<http://dx.doi.org/10.16356/j.1005-1120.2023.05.003>

scuffing incidents have occurred in the United States, Canada, Mozambique, EU member states, and other countries and regions, which resulted in aircraft damage or casualties^[3]. Although no collision incident between UAVs and aircraft has ever been reported in China, abnormal events caused by “black flight”, such as delay and cancellation of flights, aircraft route diversion, alternate landing, and even airspace closure^[4], may greatly affect the operation safety and economic benefits of air transportation, and are extremely sensitive to the public for aviation safety. According to the provisions in the Interim Regulations on the Flight Management of Unmanned Aerial Vehicles (Draft for Comments) issued by the Civil Aviation Administration of China (CAAC)^[5], the light UAVs in this work refer to remotely piloted aircraft with an empty mass of $\leq 4\ 000\text{ g}$, a maximum takeoff mass of $\leq 7\ 000\text{ g}$, and a maximum flight speed of $\leq 100\text{ km/h}$ (28 m/s).

At the design phase, the aircraft should verify the airworthiness of structural against foreign objects impact (e. g., bird strikes). However, as an emerging scenario with extensive applications, specifications of UAV design and manufacturing are still in the legal “vacuum zone”^[6]. Moreover, it is tricky to formulate universal airworthiness provisions applicable to test verification practice on the impact resistance of aircraft against UAVs. UAV operation is now supervised via relevant administrative procedures issued by the airworthiness authorities in various countries, which would be hoped to facilitate the continuous development of the UAV industry and to ensure collaborative flight safety of manned aircraft and UAVs in the same airspace simultaneously. However, collision or dangerous approaching incidents between UAVs and aircraft still usually occur, which implies to significantly investigate a risk assessment of collisions between UAVs and aircraft.

As far as the possibility of collision is concerned, several investigations on the collision hazard between UAVs and aircraft in the same airspace have been conducted, for which methods such as numerical calculation simulation and dynamic simula-

tion demonstration have been predominantly adopted. Further, the research focuses on the modeling of aircraft collision hazards based on environmental factors^[7-13], optimization of aircraft safety separations based on acceptable risks^[14-19], flight conflict avoidance, and track dynamic planning^[20-24]. However, reliable prediction models cannot be gained to assess the variation in collision risk factors, owing to the lack of comprehensive data in civil aviation regulatory authorities of various countries, such as an accurate quantity of UAV ownership, actual flight frequency, collision accident report, and the avoidance ability of aircraft. Regarding damage severity, different configurations, flight attitudes, relative speeds, impact positions, and other factors of UAVs result in great discrepancies in the severity of structural damage^[1, 2, 25]. Therefore, it is impossible to formulate a unified grading standard for UAV/aircraft damage severity. In addition to the dynamic simulation, test verification requires a long period and high cost, resulting in relatively rare achievements on the collision damage between UAVs and aircraft structural components. The main windshield on an aircraft is the largest component of windward side with great probability of being struck by foreign objects. When the load-bearing windshield glass is damaged, severe consequences will occur to the flight crew and operation. Currently, the major research works focuses on the mechanism of the collision between UAVs and aircraft windshields^[25-26], model validation^[25, 27], comparative study with bird-strike results^[28-29], and critical condition of collision damage on a windshield for a specific type aircraft^[1-2, 30-32]. According to the existing and closely related research literatures, safety and risk assessments considering both collision probability as well as damage severity of UAVs and aircraft are scarcely conducted. Most studies focuses on the collision hazard between UAVs and aircraft in the same airspace, as well as the damage from collisions between UAVs and aircraft metal structural separately. In the aforementioned cases, due to the space limit of the test apparatus, either most UAVs are simplified or collision

conditions of more severity are not considered, leading to distortion to some extent in the results.

Although the hazard analysis of UAVs ingested by aero-engines also constitutes a significant content in safety analysis of UAV crashworthiness, the research here is limited to safety and risk investigations and progress analysis of collisions between UAVs and the main windshield of aircraft. A risk matrix of collisions between UAVs and aircraft windshields is achieved by considering two dimensions including both the probability level and the damage severity rank of the collision with extreme posture of UAVs. Accordingly, the collision risk levels would be subjectively classified, and the conservative critical conditions for supervising UAV operation are determined.

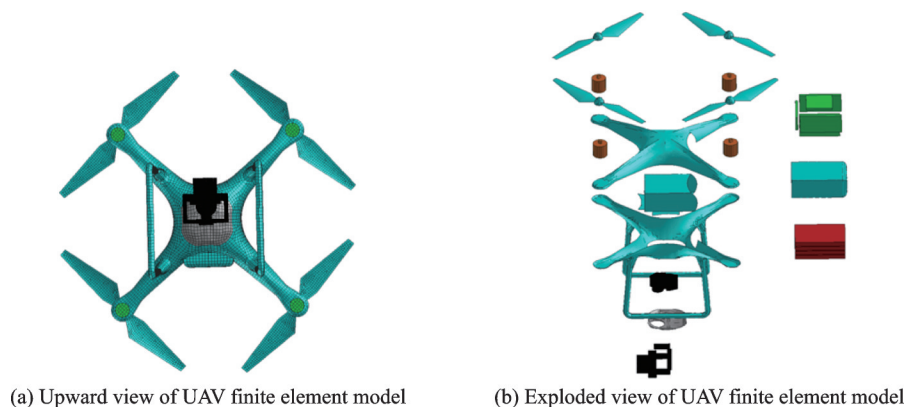








Fig.1 Configuration and major components of UAV

Table 1 Materials of major components of the UAV

Color*	Component	Material	Mass /g
	Motor	6061-T6	212
	Camera and pan-tilt	6061-T6	222
	Battery	Li-Po	459
	Circuit Board	Glass-epoxy composites	184
	Fuselage shell and blade	polycarbonate	283
	Fuselage bottom	6061-T6	
	Total		1 360

*The color of UAV components are corresponding to those labels in Fig.1.

1.2 Introduction of aircraft windshield structure

The main windshield of a commercial aircraft consists of three layers of glass and two layers of sandwich films. With edges wrapped by silicone rub-

1 Damage Rank of Collision Between UAVs and Aircraft Windshields

1.1 Introduction of UAV structure

The UAV studied here is the Phantom 4 Pro, which currently has the largest share in the market of light UAV applications. This model of UAV is produced by DJI and has been broadly adopted in laboratory investigations on collision safety in the United States, Britain, and other countries. The corresponding UAV configuration and major components are demonstrated in Fig.1, and the constructional materials of the major components are listed in Table 1. Details on UAV modeling are elaborated in Ref.[33].

ber, the three layers of glass are made of inorganic toughened materials, while the two layers of sandwich films of polyurethane (PU) and polyvinyl butyral (PVB) are constituted of organic materials. As shown in Fig.2, L1 is the outer glass which is the non-load-bearing structure with the thickness of 3 mm. L2 and L3 are the middle and inner glass, which are the load-bearing structure with thicknesses of 8 and 6 mm, respectively. PU and PVB are glue layers with thicknesses of 4 and 1.5 mm, respectively. In order to ensure the integrity of the collision simulation model, the full-size model of the aircraft nose structure including the major windshield components is exhibited in Fig.3. Details on the nose structure modeling, including the windshield, are separately elaborated in Refs.[25,33].

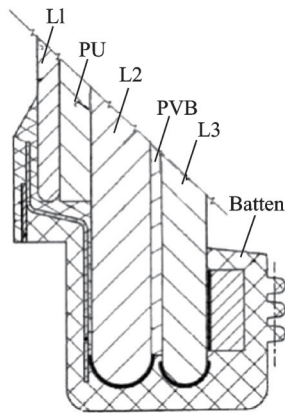


Fig.2 Section view and main components of windshield

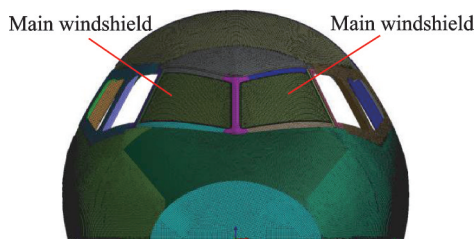


Fig.3 Model of a full-size nose of a commercial aircraft

1.3 Collision damage classification of aircraft windshields

According to the operation standards of aircraft manufacturers, a few cracks are tolerable at the outer glass of the non-load-bearing structure, as long as the vision for flight is not affected. No cracks are allowed at the middle and inner glass of the load-bearing structure. Particularly, a crack on the inner glass would threaten the equipment and personnel. Therefore, the damage rank of windshield can be successively classified into outer-layer glass crack (minor), outer-two-layer glass crack (dangerous), and three-layer glass crack (disastrous). In terms of the results of the high-speed collision between a light UAV and an aircraft windshield (same to here), acquired previously by the research team (see Ref. [25] for details), the most vulnerable position of main windshield and the harshest posture of UAV via dynamic simulations have been achieved when a UAV with the posture of pitching rearward 45° and a yawing right 24.4° along the heading direction of the aircraft struck the middle region of the windshield. As illustrated in Fig.4, the damage rank of collision between the UAV and the aircraft windshield is conservatively assessed in this case.

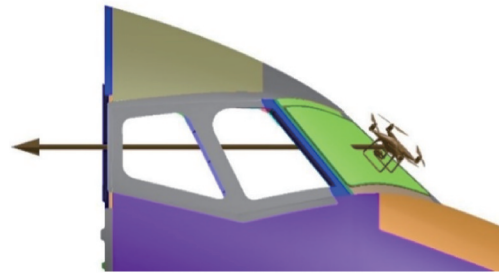


Fig.4 Impact posture of UAV and position of windshield impacted

1.4 Critical conditions of damage classification in collision simulations




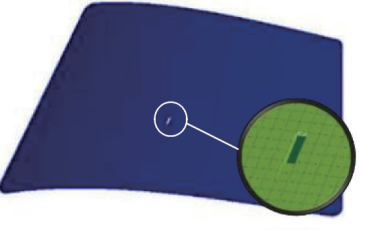


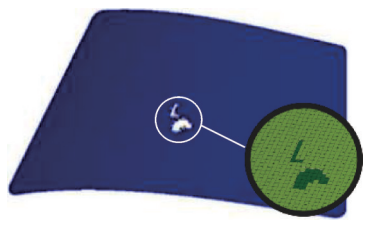


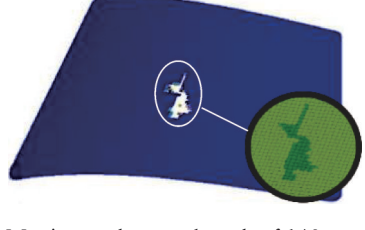
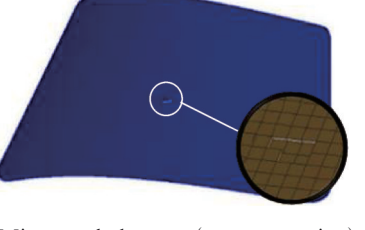

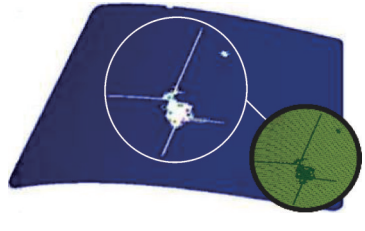
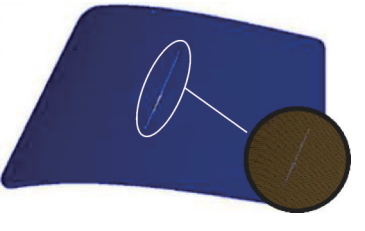

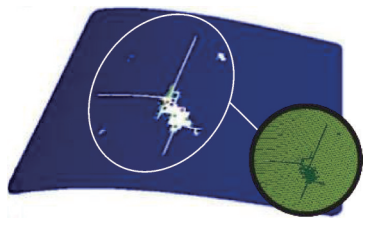
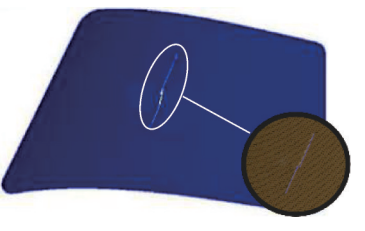
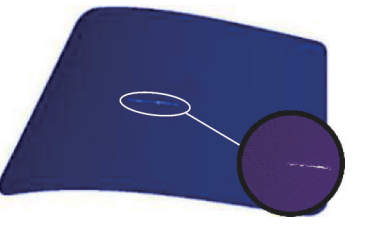
According to the existing results acquired in Ref.[25], the three layers glass had cracked entirely with the collision velocity of 151 m/s which superimposed the relative velocities of the UAV and the aircraft corresponding to the height of aircraft below 3 000 m mean sea level (MSL) to conform the FAR 91.117(a)^[34] and CCAR 91.323(a)^[35]. Therefore, by gradually decreasing the collision speed with the constant UAV flight speed of 20 m/s, the critical collision velocity corresponding to cracking in each layer glass can be obtained. Based on the aforementioned scheme, the damage of each layer glass on the windshield under typical collision conditions is listed in Table 2.

According to the simulation results in Table 2, as the UAV strikes the most vulnerable region on the windshield along the heading direction of the aircraft with the harshest posture, the conservative critical speeds of cracking of the outer layer glass, two outer layer glasses, and three layer glasses are 72 m/s, 85 m/s, and 128 m/s, respectively.

1.5 Energy level of collision between UAVs and aircraft windshields

Based on the simulation results of UAVs colliding with aircraft windshields in Section 1.4, the critical speeds and corresponding energy range of different damage classifications from the collision between a typical light UAV and an aircraft windshield under extreme condition are listed in Table 3. The damage classifications are denoted as EC1, EC2, EC3, and EC4 according to the damage extent from slight to severe.

Table 2 Damage of each layer glass on the windshield under typical collision conditions

Collision velocity*	Outer layer P1	Middle layer P2	Inner layer P3
V=70 m/s	 No damage	 No damage	 No damage
V=72 m/s	 Maximum damage length of 28 mm	 No damage	 No damage
V=80 m/s	 Maximum damage length of 91 mm	 No damage	 No damage
V=85 m/s	 Maximum damage length of 140 mm	 Microcrack damage (nonpenetrative)	 No damage
V=126 m/s	 Maximum damage length of 659 mm	 Maximum damage length of 220 mm	 No damage
V=128 m/s	 Penetrated and maximum damage length of 688 mm	 Penetrated and maximum damage length of 238 mm	 Penetrated and maximum damage length of 112 mm

* The velocity is the relative speed of UAV and aircraft.

Table 3 Damage classification of windshield impacted by UAVs

No.	UAV mass / g	Velocity range/(m · s ⁻¹)	Energy range/J	Damage degree of windshield	Damage classification
1	1 360	(0, 72]	(0, 3 525]	No damage	EC1(safety)
2		(72, 85]	(3 525, 4 913]	The outer breakage	EC2(minor)
3		(85, 128]	(4 913, 11 141]	The outer and middle breakage	EC3(dangerous)
4		(128, +∞)	(11 141, +∞)	Three breakage	EC4(catastrophic)

2 Probability Level of Collision Between UAVs and Aircraft windshields

2.1 Modelling of collision probability

The track of a commercial aircraft flying along its route is regulated in a virtual pipeline (e. g., Reich model) to eliminate track conflicts or even collisions between aircraft. The regulation involves retaining reasonably longitudinal, lateral, and vertical separations for the aircraft in the three-dimensional (3D) track pipeline. In this work, considering the short dangerous-approaching distance between UAVs and aircraft, uniform linear motion of aircraft without positioning error during the transiently approaching time is assumed. Meanwhile, in view of the relatively low flying speed of UAVs, it is regarded as a random motion particle. The motion states of the UAV and the aircraft are independent without mutual interference. On this basis, the motion models of the UAV and the aircraft in both orthogonally horizontal and vertical projection planes are established. Factors such as track alteration and conflict avoidance of UAVs and aircraft by air traffic controllers are not considered. The positional relationship between the UAV and the aircraft in the 3D orthogonal coordinate system is depicted in Fig.5.

In the 3D coordinates, points A and B indicate the positions of the aircraft and the UAV in flight space, respectively. V only indicates the space vector of the aircraft flight velocity and has no meaning of the velocity in a specific plane in Fig.5. In the initial state, the linear distance between the geometric centers of the UAV and the aircraft is D whose length in horizontal projection plane is d . Point A' is the projection of point A in the same horizontal plane including point B , and point B' is the projection of

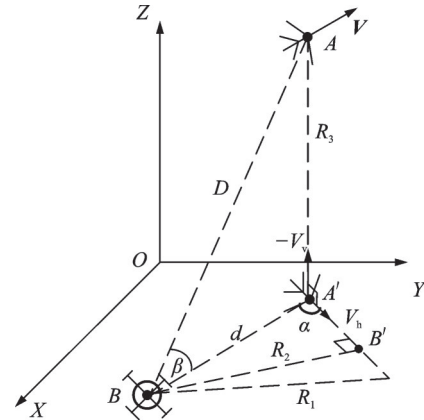


Fig.5 Space position schematics of a UAV and an aircraft

point B in the same vertical plane including point A . The relative heading angle of the aircraft to the UAV in the horizontal projection plane is $\alpha \in [-\pi, \pi]$, and the relative pitch angle of the aircraft to the UAV in the vertical projection plane is $\beta \in [-\pi/2, \pi/2]$. The motion of UAV is simplified as Gaussian distribution in the horizontal and vertical projection planes, and the various uniform horizontal motions of the aircraft in different flight phases and the single uniform vertical motion in multiple flight phases are assumed. Considering the size effects of the UAV and the aircraft, the volume parameters (length \times width \times height) of the UAV and the aircraft are assumed as $a_1 \times b_1 \times c_1$ and $a_2 \times b_2 \times c_2$, respectively. Therefore, the spacing errors in the horizontal and vertical projection planes resulting from the volume parameters of the UAV and the aircraft are

$$\begin{cases} \Delta_h = \sqrt{a_1^2 + b_1^2} + \sqrt{a_2^2 + b_2^2} \\ \Delta_v = |c_1| + |c_2| \end{cases} \quad (1)$$

At time t from the initial state, the random dynamics differential equations of the UAV and the aircraft in the horizontal projection plane are given by

$$\begin{cases} dL(t) = V_h(t)dt + U_h(t)dt \\ L(0) = 0 \end{cases} \quad (2)$$

where $L(t)$ and $L(0)$ are the horizontal distance of

aircraft having flown relative to UAV at time t and at the start time, respectively; $V_h(t)$ is the various average velocity of the aircraft in the horizontal projection planes corresponding to different flight phases; $U_h(t)$ is the horizontal velocity of the UAV in standard Gaussian motion with $E[U_h(t)] = 0$ and $D[U_h(t)] = \sigma_h^2$, in which the value of σ_h^2 is determined by the horizontal velocity of the UAV. Therefore, the distance $R_1(t)$ between the UAV and the aircraft in the horizontal projection plane at time t from initial state can be expressed as

$$\begin{cases} R_1(t) = \sqrt{(L(t))^2 + d^2 - 2 \times L(t) \times d \times \cos \alpha} - \Delta_h \\ d = D \times \cos \beta \end{cases} \quad (3)$$

According to Fig.5, the lateral distance $R_2(t)$ of the UAV relative to the aircraft heading in the horizontal projection plane can be written as

$$R_2(t) = d \times |\sin \alpha| - |b_1| - |b_2| \quad (4)$$

In the horizontal projection plane, if the horizontal distance $R_1(t)$ or the lateral distance $R_2(t)$ is less than the specified minimum safety separation, it is considered that collision has occurred between the UAV and the aircraft in the horizontal plane.

At time t from the initial state, the random dynamics differential equations of the UAV and the aircraft in the vertical projection plane are given by

$$\begin{cases} dH(t) = V_v(t) dt + U_v(t) dt \\ H(0) = 0 \end{cases} \quad (5)$$

where $H(t)$ and $H(0)$ are the vertical distance of aircraft having flown relative to the UAV at time t and at the start time, respectively; $V_v(t)$ is the single average velocity of the aircraft in the vertical projection planes in multiple flight phases; $U_v(t)$ is the vertical velocity of UAV in standard Gaussian motion with $E[U_v(t)] = 0$ and $D[U_v(t)] = \sigma_v^2$, in which the value of σ_v^2 is determined by the vertical velocity of the UAV. Hence, the distance $R_3(t)$ between the UAV and aircraft in the vertical projection plane can be expressed as

$$\begin{cases} R_3(t) = H - H(0) \\ H = D \times \sin \beta - \Delta_v \end{cases} \quad (6)$$

where H is the vertical distance between the UAV and the aircraft at the start time. If $R_3(t)$ is less than

the specified minimum safety separation, it is considered that collision has occurred between the UAV and the aircraft in the vertical plane.

2.2 Solution of collision probability model

R'_1 , R'_2 , and R'_3 are adopted to represent the horizontal, lateral, and vertical safety separations, respectively. Within the total time of $t = k \times \Delta t$ (where k is the step number of time increments), the decisive indicators for the collision between the UAV and the aircraft regarding the horizontal, lateral, and vertical distance, i.e., f_1 , f_2 , and f_3 , are defined as

$$\begin{cases} f_1 = 0 & R_1 \leq R'_1 \\ f_1 = 1 & R_1 > R'_1 \end{cases} \quad (7)$$

$$\begin{cases} f_2 = 0 & R_2 \leq R'_2 \\ f_2 = 1 & R_2 > R'_2 \end{cases} \quad (8)$$

$$\begin{cases} f_3 = 0 & R_3 \leq R'_3 \\ f_3 = 1 & R_3 > R'_3 \end{cases} \quad (9)$$

At time t , when $((f_1 = 0 \text{ or } f_2 = 0) \& f_3 = 0)$ is fulfilled with $\alpha \in [-\pi/2, \pi/2]$ or $(f_1 = 0 \& f_3 = 0)$ is fulfilled with $\alpha \in [-\pi, -\pi/2]$ and $\alpha \in [\pi/2, \pi]$, it is considered that collision occurs between the UAV and the aircraft in 3D space. With a total simulation times, the simulation flowchart, presented in Fig.6, is determined according to the schemes in Sections 2.1 and 2.2.

2.3 Simulation results of collision probability

According to the introduction in Section 2.1, the related parameters of the UAV and the aircraft used in the simulation of collision probability are listed in Table 4. The UAV can reach the maximum height from the ground of 500 m in terms of the design performance. Now, the permissible flight height of the UAV is 120 m due to flight control. Meanwhile, as the flight speed range of the UAV is small, the UAV can promptly attain a stable speed and be simplified a random particle motion. However, the speed range of the aircraft varies greatly from taxiing to cruising with different flight speeds in various flight phases, corresponding to which different average horizontal flight speed in each phase should be defined. The average horizontal velocities of the aircraft in Table 4

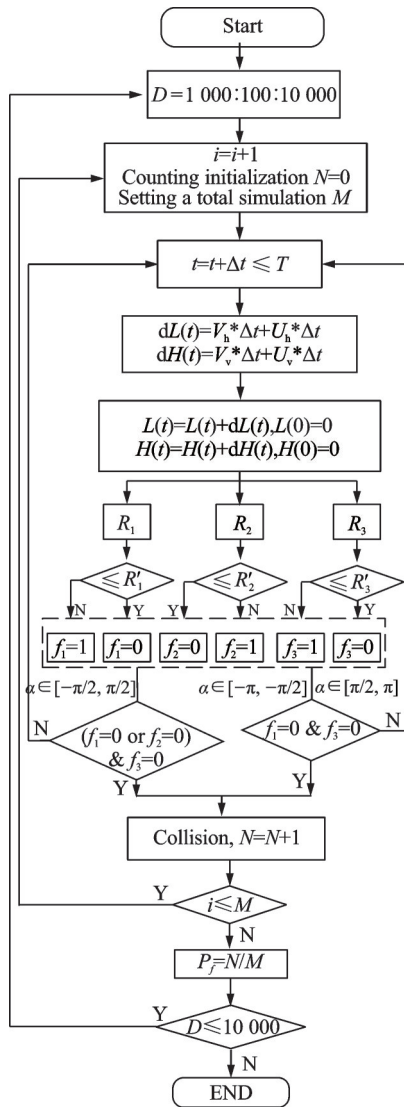


Fig.6 Numerical simulation flowchart of collision probability

are compared with the critical collision speeds in Table 2 that cause cracking in

turn, which indicates that the critical collision speed resulting in cracking of all three layers glass of the windshield corresponds to a height range of 120—500 m and climbing stage of aircraft according to its flight performance and speed envelope. Without consideration of flight control, a collision between the UAV and the aircraft would be very likely to happen. Therefore, collision simulation of the aircraft with the speed of 108 m/s (deriving from (128−20) m/s) is considered conservatively here. Likewise, the critical collision speed at which the outer-two layers glass of the windshield cracked corresponds to a height range below 120 m and taking off stage of aircraft, in which the collision risk between the UAV and the aircraft would really exist. Therefore, three critical velocities of the aircraft that cause cracking of each layer glass of the windshield in turn, i.e., 52 m/s, 65 m/s, and 108 m/s, are considered in the simulation.

With reference to relevant technical documents and literatures^[36-37], the selected parameters in the simulation for flight safety separation in the aircraft terminal control area are listed in Table 5.

Assuming $D = 10\ 000$ m, the collision probabilities with various combinations of α and β in their ranges and velocity of 128 m/s are displayed in Fig.7. It is clearly showed that the collision probability between the aircraft and the UAV would reach the maximum when α and β are equal to zero, which is also in conformity with the common sense.

Table 4 Horizontal and vertical speeds of different models

Model	The length, width and height of the body/m	Average vertical velocity*/(m · s ⁻¹)	Average horizontal velocity*/(m · s ⁻¹)
PHANTOM 4	0.289, 0.289, 0.196	5	20
A commercial aircraft	3.346, 3.042, 4.170	2	52 (Corresponding to the speed of taxiing and taking off) 65 (Corresponding to the speed of taking off stage and the max speed of a height of about 120 m) 108 (Corresponding to the speed of climbing stage and the max speed of a height of about 500 m)

* The aircraft speed refers to it in its ascending process with the maximum takeoff weight. Generally, the speed in the ascending process is greater than that in the descending process at the same flight height. Therefore, conservative values are selected. The customized maximum flight height of the UAV is 500 m which is more than that of the critical flying height of aircraft corresponding to various damage classifications of windshield.

Table 5 Safety separation parameters in the simulation

Parameter	Value
Minimum horizontal safety interval R'_1/m	2 000
Minimum lateral safety interval R'_2/m	1 000
Minimum vertical safety interval R'_3/m	100

Based on Fig.7 and previous study^[37], the typical scenario of α and β being equal to 30° is considered to conservatively estimate the risks of dangerous approaching and collision between the aircraft and UAV without considering any avoidance strategies.

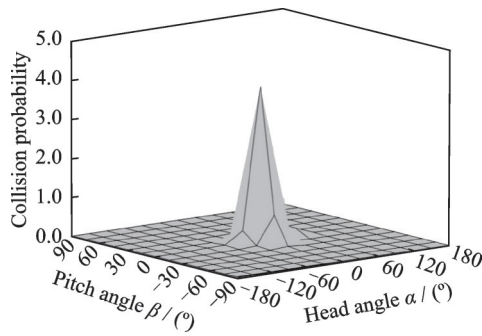


Fig.7 Collision probability of combination with various angles

The relationship in the collision probability and the initial space distance D between the aircraft and UAV are displayed in Fig.8. The SAE ARP 4761 standard^[38] is cited by the Coordination Working Group on General Structure of Transport Airplanes in FAA Aviation Rulemaking Advisory Committee. Qualitative and quantitative safety indicators including the consequences of different failure modes, the severity classification of failure states, and the acceptable probability of occurrence defined by Federal Aviation Administration (FAA) and Joint Aviation Authorities (JAA) are adopted in the cited standard: (1) The adverse effects, which slightly reduce the safety margin, slightly increase the workload of the flight crew, or render certain inconvenience on the passengers, fall into the category of minor damage or failure conditions with an allowable occurrence frequency as quite likely and an occurrence probability of $\leq 10^{-3}$; (2) the adverse effects, which notably reduce the safety margin or

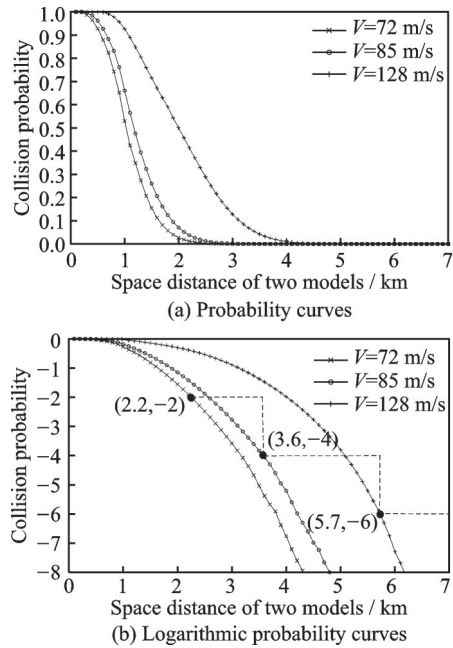


Fig.8 Relationship between spatial distance and collision probability of UAV and aircraft with different speeds

functional capability, notably increase the workload of the flight crew, affect the crew efficiency, or render certain discomfort on the passengers, fall into the category of hazardous damage or failure conditions with an allowable occurrence frequency as seldom and an occurrence probability of $\leq 10^{-5}$; (3) the adverse effects, which greatly reduce the safety margin or functional capability, impose greater workload and physical pain on the flight crew that cannot execute tasks accurately and completely, or adversely impact the passengers, fall into the category of severe damage or failure conditions with an allowable occurrence frequency as rare and an occurrence probability of $\leq 10^{-7}$. According to the aforementioned indicators of damage and safety, the spatial distance and collision probability between the UAV and the aircraft corresponding to the windshield damage classification with different collision conditions listed in Table 3 are depicted by the three solid curves corresponding to different marks in Fig.8, assuming that cases in which the UAV strikes the aircraft windshield accounts for 10% of the total collision incidents between UAVs and aircraft referring to the 30-year statistical results (about 15%) of birds striking the aircraft windshield^[39].

To unify the variation relations between spatial distance and collision probability of the UAV and the aircraft with different speeds, the dotted line of collision probability in Fig.8(b) is obtained in view of conservative safety targets. Thereby, the collision probability level is classified to acquire the cor-

responding probability ranges of collision for the aircraft windshield. The probability classification are denoted as PC1, PC2, PC3, and PC4 according to the probability magnitude from low to high and the range divisions corresponding to each level of collision probability are presented in Table 6.

Table 6 Probability interval corresponding to possible collision level

Classification of collision possibility	Space distance range between two models/m	Collision probability* range
PC1	[5 700, $+\infty$)	(0, 10^{-7}]
PC2	[3 600, 5 700)	(10^{-7} , 10^{-5}]
PC3	[2 200, 3 600)	(10^{-5} , 10^{-3}]
PC4	[0, 2 200)	(10^{-3} , 1]

*The probability includes the assumed 10% proportion for a UAV striking a windshield of the total collision incidents.

3 Collision Risk Between UAVs and Aircraft Windshields

Referring to the Guidelines for Risk Assessment of Airworthiness Certification Projects of Civil UAV Systems (Trial)^[40], two indicative dimensions, i.e., probability level and damage rank, are selected to express the collision risk of a typical UAV and a commercial aircraft windshield. According to the results shown in Tables 3, 6, the colli-

sion risk matrix for the UAV and the aircraft flying in the same sub-air-space with both pitch angle and heading angle of 30° is exhibited in Table 7. The yellow zone indicates low risk (R_1), the orange zone indicates medium risk (R_2), and the red zone indicates high risk (R_3). Therefore, in terms of different acceptable risk zones, the corresponding ranges of collision energy and the unregulated spatial distance between the UAV and the aircraft can be determined reversely.

Table 7 Collision risk matrix between typical light UAV and windshield of an aircraft

Classification of damage severity	PC1 [5 700, $+\infty$) (0, 10^{-7}]	PC2 [3 600, 5 700) (10^{-7} , 10^{-5}]	PC3 [2 200, 3 600) (10^{-5} , 10^{-3}]	PC4 [0, 2 200) (10^{-3} , 1]
EC1 (0, 3 525) No damage	R_1	R_1	R_2	R_3
EC2 [3 525, 4 913) The outer breakage	R_1	R_2	R_3	R_3
EC3 [4 913, 11 141) The outer and middle breakage	R_2	R_3	R_3	R_3
EC4 [11 141, $+\infty$) Three breakage	R_2	R_3	R_3	R_3

4 Conclusions

The collision probability and energy levels corresponding to various damage severity ranks of a typical light UAV and a commercial aircraft windshield during flying in the same sub-air-space at a certain altitude are analyzed. With the lack of further test verifications and sufficient supports from simula-

tion results regarding more actual conditions, the results can provide conservative but rational understandings of collision risks between UAVs and aircraft. The following conclusions can be drawn.

(1) If the distance between the UAV and the aircraft is more than 3 600 m before the aircraft takes off corresponding to the energy level EC1 of impacting, or more than 5 700 m under the flight

height of 120 m corresponding to the energy level EC2 of impacting, the collision probability and damage severity are acceptable in general, which means low risk.

(2) If the distance between the UAV and the aircraft is greater than 2 200 m before takeoff corresponding to the energy level EC1 of impacting, more than 3 600 m under the flight height of 120 m corresponding to the energy level EC2 of impacting, or more than 5 700 m above the flight height of 120 m corresponding to the energy level EC3 of impacting, the collision probability and damage severity present great risks, which means moderate risk and that avoidance measures should be taken for the mitigation.

(3) If the distance between the UAV and the aircraft is less than 2 200 m before takeoff corresponding to the energy level EC1 of impacting, less than 3 600 m under the flight height of 120 m corresponding to the energy level EC2 of impacting, or less than 5 700 m above the flight height of 120 m corresponding to the energy level EC3 or EC4 of impacting, the collision probability and damage severity indicate grave risks, which means high risk and measures like electronic fences or conflict alerts should be taken to avoid collision incidents.

(4) It has been studied that the windshield was impacted respectively by the UAV and a four-pound bird with the same kinetic energy in Ref.[25]. The results showed that there was no damage to the windshield when the bird impacted the windshield at a speed of 132.7 m/s. Therefore, combined with the achievements in this paper, the windshield of the aircraft is safe after being impacted by a four-pound bird below 500 m.

This work provides a conservative method for risk assessment of mid-air collisions between a typical light UAV and commercial aircraft windshield. Because of the incomplete information on the existing UAV products registered in official website of Civil Aviation Administration of China (CAAC) as well as the lack of statistical information on the collision incidents between UAVs and aircraft, the energy distribution function of collisions with various models of UAV cannot be obtained, and the pro-

posed collision probability model is a little imperfect. Therefore, the accuracy of quantitative analysis and the rationality of the risk assessment matrix for collisions between UAVs and aircraft windshields require further improvement. In general, the results of this study provide a significant insights for engineering practices in the normative design of the light UAV industry. Additionally, these findings can offer open referential effects on the decision-making for the civil aviation regulatory authorities.

References

- [1] GERARDO O, THOMAS L, LUIS G, et al. UAS airborne collision severity evaluation, final report volume I[R]. Springfield, USA: [s.n.], 2017: 11-18.
- [2] GERARDO O, LUIS G, JAIME E, et al. UAS airborne collision severity evaluation- quadcopter, final report volume II [R]. Springfield, USA: [s. n.] , 2017:8-128.
- [3] LIU Xinchao. Simulation and safety assessment of collisions between drones and civil aircraft[D]. Nanjing: Nanjing University of Aeronautics and Astronautics, 2019: 1-3. (in Chinese)
- [4] QUAN Quan, LI Gang, BO Yiqin, et al. Low altitude UAV traffic management: An introductory overview and proposal[J]. Acta Aeronautica et Astronautica Sinica, 2022, 41(1): 6-34. (in Chinese)
- [5] Civil Aviation Administration of China. Interim Regulations on the Flight Management of Unmanned Aerial Vehicles (Draft for Comments) [EB/OL]. (2018-01-26). http://www.caac.gov.cn/HDJL/YJZJ/201801/t20180126_48853.html.(in Chinese)
- [6] LUAN Shuang. On basic problems of civil UAV legal regulation[J]. Journal of Nanjing University of Aeronautics and Astronautics (Social Sciences) , 2018, 20(2): 54-58. (in Chinese)
- [7] WANG Songtao, LV Zongping, ZHANG Zhaoning. Study of the collision risk model involving flight environment conditions under free flight[J]. China Science-paper, 2016, 11(19): 2183-2186. (in Chinese)
- [8] LI Qi, GAN Xusheng, SUN Jingjuan, et al. Risk assessment of lateral collision between military UAV and civil aviation flight[J]. Journal of Beijing University of Aeronautics and Astronautics, 47(4): 724-730. (in Chinese)
- [9] MCFADYEN A, MARTIN T, PEREZ T. Low-level collision risk modelling for unmanned aircraft integration and management[C]//Proceedings of the 2018 IEEE Aerospace Conference.[S.l.]: IEEE, 2018: 946-955.

- [10] COUR-HARBO A L, SCHIOLER H. Probability of low-altitude midair collision between general aviation and unmanned aircraft[J]. *Risk Analysis*, 2019, 39(11): 2499-2513.
- [11] LEE S S. Statistical mid-air collision risk assessment[D]. Canada: Memorial University of Newfoundland, 2021: 88-118.
- [12] XIA C Y, YANG C R, XUE K, et al. A conflict risk analysis of MAV\UAV flight in shared airspace[J]. *International Journal of Aerospace Engineering*, 2021. DOI: 10.1155/2021/1692896.
- [13] KALLINEN V, MCFADYEN A. Collision risk modeling and analysis for lateral separation to support unmanned traffic management[J]. *Risk Analysis*, 2021, 42(4): 854-881.
- [14] YANG Min. Safety risk assessment of collision between UAV and civil aircraft[D]. Guanghan: Civil Aviation Flight University of China, 2019: 32-62. (in Chinese)
- [15] WEI Ahui. Research on flight separation assessment method based on space-based ADS-B[D]. Tianjin: Civil Aviation University of China, 2020: 14-20. (in Chinese)
- [16] MA X, ZHANG X, WANG H, et al. An operational safety evaluation method for manned transport aircraft and large UAV in mixed airspace[J]. *Mathematical Problems in Engineering*, 2021. DOI: 10.1155/2021/6636794.
- [17] CHEN C, EDWARDS M W, GILL B, et al. Defining well clear separation for unmanned aircraft systems operating with noncooperative aircraft[C]//Proceedings of AIAA Aviation 2019 Forum. Dallas, USA: AIAA, 2019: 1-21.
- [18] RAMASAMY S, SABATINI R, GARDI A. A unified analytical framework for aircraft separation assurance and UAS sense-and-avoid[J]. *Journal of Intelligent & Robotic Systems*, 2018, 91(3/4): 735-754.
- [19] DU Y, ZHANG X, GU Q. Adaptive separation thresholds for self-separation of unmanned aircraft system in dynamic airspace[J]. *IEEE Access*, 2019(7): 141817-141825.
- [20] YANG Jianhang, ZHANG Fubiao, WANG Jiang. Conflict resolution algorithms for UAV low-altitude flight based on reachable set[J]. *Journal of Beijing University of Aeronautics and Astronautics*, 2023, 49(7): 1813-1817. (in Chinese)
- [21] HUANG Yang, TAGN Jun, LAO Songyang. UAV flight conflict resolution algorithm based on complex network[J]. *Acta Aeronautica et Astronautica*, 2018, 39(12): 262-274. (in Chinese)
- [22] SEUNGWON N. Methodology for collision risk assessment of aircraft with diverse collision avoidance capabilities[D]. Fairfax, USA: George Mason University, 2020: 40-70.
- [23] KHAN A. Risk assessment, prediction, and avoidance of collision in autonomous drones[C]//Proceedings of 17th European Dependable Computing Conference (EDCC 2021). Munich, Germany: [s.n.], 2021: 1-4.
- [24] GUAN X, LYU R, Shi H, et al. A survey of safety separation management and collision avoidance approaches of civil UAS operating in integration national airspace system[J]. *Chinese Journal of Aeronautics*, 2020, 33(11): 2851-2863.
- [25] LU X, LIU X, LI Y, et al. Simulations of airborne collisions between drones and an aircraft windshield[J]. *Aerospace Science and Technology*, 2020, 98(9): 105713.
- [26] CHOI Y, LEE S, JUNG J, et al. Collision mechanism of unmanned aerial vehicles onto glass panels [J]. *International Journal of Micro Air Vehicles*, 2021, 13: 1-18.
- [27] WU Zhijian. Numerical study on dynamic response and damage of the UAV impact civil aircraft[D]. Guanghan: Civil Aviation Flight University of China, 2018: 21-33. (in Chinese)
- [28] LIU Jijun, LIU Xiaochuan, GUO Jun. Comparative study on impact of small UAV and bird on aircraft windshield[C]//Proceedings of the 6th International Unmanned Aerial Vehicle System Conference of China. Beijing, China: [s.n.], 2016: 67-72. (in Chinese)
- [29] GUO Yazhou, LIU Xiaochuan, GUO Jun, et al. Comparative experiment of aircraft windshield glass subjected to micro-UAV and bird body impact[J]. *Journal of Experimental Mechanics*, 2020, 35(1): 167-173. (in Chinese)
- [30] MAN M, LOW K H. Damage severity prediction of helicopter windshields caused by a collision with a small unmanned aerial vehicle (sUAV)[C]//Proceedings of AIAA Aviation 2021 Forum. [S.l.]: AIAA, 2021: 1-11.
- [31] ALEXANDER R. Potential damage assessment of a mid-air collision with a small UAV[D]. Melbourne, Australia: Monash University, 2013: 9-17.
- [32] The Department For Transport, The Military Aviation Authority. Small remotely piloted aircraft systems (drones) mid-air collision study: TW9 4DU[R]. Kew, UK: [s.n.], 2016: 9-16.
- [33] LU X, LIU X, ZHANG Y, et al. Simulation of airborne collision between a drone and an aircraft nose[J]. *Aerospace Science and Technology*, 2021, 118: 107078.

- [34] Federal Aviation Administration. 14 CFR Part 91—General operating and flight rules (Amendment NO: 91-233)[S]. Washington D C, USA: 1993.
- [35] Civil Aviation Administration of China. General operating and flight rules (CCAR -25-R4) [S]. Beijing, China: 2022. (in Chinese)
- [36] U.S. Department of Transportation, Federal Aviation Administration. Aeronautical information manual-official guide to basic flight information and ATC procedures[M]. Washington DC, USA: [s.n.], 2014.
- [37] DENG Li. Research of collision probability of unmanned aerial vehicles and civil airplane[J]. Journal of Nanjing University of Science and Technology, 2019, 43(1): 122-128. (in Chinese)
- [38] Society of Automotive Engineers, Inc. Guidelines and methods for conducting the safety assessment process on civil airborne system and equipment, ARP 4761 [S]. [S.l.]: [s.n.], 1996.
- [39] RICHARD A D, MICHAEL J B, PHYLLIS R M, et al. Wildlife strikes to civil aircraft in the United States, 1990—2019[R]. Washington DC, USA: [s.n.], 2021.
- [40] Airworthiness Certification Department of CAAC. The guidelines for risk assessment of airworthiness certification projects of civil UAV systems (Trial)(No. [2020] 9)[S]. Beijing, China:[s.n.], 2018. (in Chinese)

Acknowledgement This work was supported by the Na-

tional Natural Science Foundation of China (No.71971114).

Authors Mr. ZHANG Zhuguo is a Ph. D. candidate of Northwestern Polytechnic University. Now he is in the employment of Shanghai Aircraft Airworthiness Certification Center as a senior engineer. His research interests focus on airworthiness certification of transport aircraft structure, aircraft design and digital twin technology.

Dr. LU Xiaohua received his Ph.D. degree from Nanjing University of Aeronautics and Astronautics(NUAA). His research is focused on aviation maintenance engineering, prognostics health management, damage assessment and impact dynamics.

Author contributions Dr. ZHANG Zhuguo simulated partial collision conditions, established the theoretical model of collision probability, designed the two-dimensional risk matrix, and wrote the manuscript. Dr. LU Xiaohua built the finite element models of UAV and aircraft, participated in partial impact simulation, and contributed to the background introduction. Mr. ZHANG Yingchun interpreted relevant airworthiness documents, proposed collision risk indexes, and provided a few cases about background of the study. Prof. LI Yulong contributed to guide modeling and simulation of collision, and discussed the conclusion. Prof. ZHANG Honghai contributed to the simulation process optimization of collision probability. All authors commented on the manuscript draft and approved the submission.

Competing interests The authors declare no competing interests.

(Production Editor: ZHANG Bei)

轻型无人机与飞机风挡碰撞风险研究

张柱国^{1,3}, 陆晓华², 张迎春³, 李玉龙¹, 张洪海²

(1. 西北工业大学航空学院, 西安 710072, 中国; 2. 南京航空航天大学民航学院, 南京 211106, 中国;

3. 中国民航上海航空器适航审定中心, 上海 200335, 中国)

摘要: 随着无人机应用的快速增长, 机场附近和空域已发生了很多重大航空事故和危险征候, 无人机的无序飞行对航空运输安全构成了巨大的潜在威胁。以典型轻型无人机和某型商用飞机及其风挡为研究对象, 通过有限元仿真方法得到无人机在最严酷姿态下与飞机风挡最薄弱位置碰撞损伤等级及相应的冲击能量区间, 以此保守划分损伤严重性等级。在无空中交通指挥干预的情况下无人机与飞机相互独立运动, 考虑两机之间的水平最小安全间隔、侧向最小安全间隔以及垂直最小安全间隔的联合约束, 通过蒙特卡洛仿真得到无人机与飞机的碰撞概率, 并确定碰撞可能性等级。基于损伤严重性等级和碰撞可能性等级的不同组合形成无人机与飞机风挡碰撞的较为保守的定性风险矩阵。研究结果总体表明: 在 120 m 飞行高度下, 两机距离超过 3 600 m 且在典型的俯仰角和航向角工况下发生碰撞风险及其损伤程度较小, 否则发生碰撞风险较大且损伤程度较严重。研究结果为无人机的规范性设计制造、局方对无人机运行管控的政策制定以及无人机与载人飞机在同一空域运行的风险评估提供理论依据和实践参考。

关键词: 无人机; 飞机风挡; 碰撞概率; 损伤严重性; 能量等级; 风险矩阵